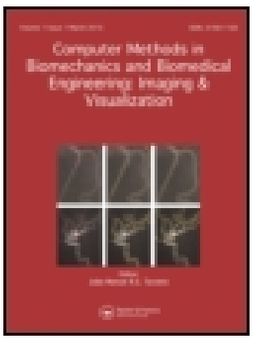

Taylor & Francis
Taylor & Francis Group

Computer Methods in Biomechanics and Biomedical Engineering: Imaging & Visualization

ISSN: 2168-1163 (Print) 2168-1171 (Online) Journal homepage: https://www.tandfonline.com/loi/tciv20

Using 3D anthropometric data for the modelling of customised head immobilisation masks

MAR Loja, E Sousa, L Vieira, DMS Costa, DS Craveiro, R Parafita & DC Costa

To cite this article: MAR Loja, E Sousa, L Vieira, DMS Costa, DS Craveiro, R Parafita & DC Costa (2019): Using 3D anthropometric data for the modelling of customised head immobilisation masks, Computer Methods in Biomechanics and Biomedical Engineering: Imaging & Visualization

To link to this article: https://doi.org/10.1080/21681163.2018.1507840

Published online: 04 Apr 2019.

COMPUTER METHODS IN BIOMECHANICS AND BIOMEDICAL ENGINEERING: IMAGING & VISUALIZATION
https://doi.org/10.1080/21681163.2018.1507840

Using 3D anthropometric data for the modelling of customised head immobilisation masks

MAR Loja [a,b,c], E Sousa [a,d], L Vieira [a,d,e], DMS Costa [a], DS Craveiro [a,b], R Parafita [f,g] and DC Costa [f]

[a]GI-MOSM, ADEM, ISEL - Grupo de Investigação em Modelação e Optimização de Sistemas Multifuncionais, Lisboa, Portugal; [b]ISEL - Instituto Superior de Engenharia de Lisboa, Lisboa, Portugal; [c]H&TRC - Health &Technology Research Center, ESTeSL/IPL - Escola Superior de Tecnologia da Saúde de Lisboa/Instituto Politécnico de Lisboa, Lisboa, Portugal; [d]Instituto de Biofísica e Engenharia Biomédica, Faculdade de Ciências da Universidade de Lisboa, Lisboa, Portugal; [e]Nuclear Medicine-Radiopharmacology, Champalimaud Centre for the Unknown, Champalimaud Foundation, Lisboa, Portugal; [f]Nuclear Medicine Sector, Mercurius Health, Lisboa, Portugal; [g]LAETA, IDMEC, Instituto Superior Técnico, Universidade de Lisboa, Lisboa, Portugal

ABSTRACT

Head immobilization thermoplastic masks for radiotherapy purposes involve a distressful modelling procedure for the patient. To assess the possibility of using different acquisition and reconstruction methods to obtain a 3Dskin surface model of PIXY-phantom-head and to present a proposal of an alternative head immobilisation mask prototype. Phantom head geometry acquisitions using: computed tomography (reconstructed with ImageJ and Osirix); and 3DLaserScanner (reconstructed with SolidWorks). From these reconstructed surface models a set of landmarks was measured and subsequently compared with physical measurements obtained with a Rosscraft-Calliper. For statistical evaluation, relative deviations graphics and Friedman-test for non-parametrical paired samples were used, with a significance level of 5%. For a first assessment of the proposed mask performance, a radiotransparent material was considered, the strength and stiffness evaluation being performed using the finite element method. There are small differences between all the acquisitions and reconstructions methods and the physical measurements, statistically significant differences (X2F(6)) = 6.863, p=0.334) were not found. The proposed mask performed well from the strength and stiffness perspectives, leading to the desired immobilisation aim. The immobilisation mask design proposal may be an effective alternative to the present completely hand-made situation, which presents a high-degree of discomfort and stress to the patients.

ARTICLE HISTORY
Received 29 July 2017
Accepted 1 August 2018

KEYWORDS
3D surfaces scanning; computed tomography; computational modelling of head surface; immobilisation mask prototype; mask' mechanical behaviour

1. Introduction

The measurement of people physical parameters and proportions constitutes an important field of science as it enables the understanding of anthropological information associated to human, an improved knowledge of our ancestors' heritage and the improvement in design and sizing of systems and devices to human use.

This problem is especially complex in non-rigid applications. To use these models in such applications, approaches are required to extract anthropometric data from human body scans. The extracted measures build the basis for further processing and thus automatic and reliable approaches are important.

The literature proposes semi-automatic and automatic approaches like detecting landmarks and their precise localisation, although other methods recurring to new developed algorithms and prior data enable the model of 3D surface without recurring to landmarks as done by Anguelov et al. ([date unknown]). Nowadays, several acquisition methods and equipment are available, ranging from low-cost scanners to professional and more expensive scanning equipment that can be used to reconstruct precise 3D models of a human body.

Within the more accessible methods to acquire 3D surfaces, one can refer 3D scanners or computed tomography (CT) technique, CT being the gold standard, as it constitutes currently the main imaging technique to assess surface for radiotherapy in clinical application. The work developed by Gopan and Wu (2012) and by Morton (2011) illustrates this, by focusing on the accuracy issues related to CT imaging technique.

The advent of more complex CT imaging systems has posed an increasing challenge in our ability to assess their performance, including spatial resolution. The evaluation of spatial resolution for the applied imaging systems is essential to obtain accurate and precise measurements. Richard et al. (2012) addressed the problem associated to iterative and statistical reconstructions which can exhibit nonlinear signal characteristics, affecting system resolution properties differently than with standard acquisition techniques and reconstruction algorithms.

The usual method of three-dimensional reconstruction in OsiriX is rendering by volume from a three-dimensional dataset that comprises a piled group of flat two-dimensional images. These images are acquired in sequence, with a standardised distance between each and with a regular number of two-dimensional pixels. To create volume rendering, a camera is placed virtually relative to the space created and all voxels

CONTACT L Vieira lina.vieira@estesl.ipl.pt Escola Superior de Tecnologia da Saúde de Lisboa, Instituto Politécnico de Lisboa, Av. D. João II, Lote 4.69.01 1990 – 096, Lisboa, Portugal

contain information on colour and transparency. Surface rendering can be accomplished using a number of different algorithms and consists of a process by which three-dimensional data are converted into vector models. These models are made up of vertices, lines and planes. The conversion is dependent on the algorithm chosen, on the structure to be converted and on the cut-off point chosen (Amato 2017). Also, ImageJ can be used for 3D reconstruction and rendering in the creation of 3D surfaces for medical images although ImageJ was developed with 2D processing and analysis in mind, thanks to plugins, it became a powerful software for 3D processing and analysis (Andrey and Boudier [date unknown]). SurfaceJ is a plugin to create surface plots. Surface plots are colour-coded 3D renderings of the intensity information in the image, where the height (on the z-axis) and the colour in the rendering correlate with the intensity of a pixel in the image (Abramoff and Viergever 2002).

Contrarily to CT, made of a sequence of bi-dimensional images, 3D laser scanning (3DLS) provides a three-dimensional sampling of an object, namely of the human body, characterising it by a dense set of points in the 3D space, usually known as point's cloud. The topology of these points can be represented, for instance, through the constitution of a polygonal mesh or via parametric surfaces. It is noteworthy that the measurements obtained represent the human body at a certain time and that various scans may lead to slightly different results, as pointed by Paquet and Rioux (2003).

Recent advances in three-dimensional scanning technology have enabled the generation of high-density point data sets to describe the surfaces of real objects (Bernardo et al. 2016; Bernardo and Loja 2017), including animate objects such as the human body. This means that it is now possible to produce computer-based models that describe in detail the topology and the geometry of an actual human body. Such models can be used to perform fast and accurate automatic measurements. However, such measurements cannot be made on raw point data, as very often the point's cloud is noisy and contains undesired information. To minimise these problems, Douros et al. (1999) proposed an algorithm to analyse the data and from it infer the topology (and subsequently the geometry), taking into consideration that skin surface presents further challenges, such as more accurate reconstruction algorithms.

The clinical applications for these anthropometric measurements acquisitions and models are innumerous, being the most known in the field of prosthetic applications. Nowadays, these clinical applications are still in an accentuated increase due to the growing availability of the 3D printing (Dodziuk 2016).

On the other side, some of the medical fields could greatly benefit from the design of immobilisation devices with the same principles and techniques and this is still not fully available yet (Head, Neck and Shoulders Immobilization Systems [date unknown]; Arino et al. 2014).

Brain imaging that requires a long time of immobilisation or head and neck radiotherapy imposes the need for immobilisation systems to provide an effective degree of rigidity, together with an acceptable degree of comfort for the patient. However, actually, the more clinically widely diffused creation process that involves thermoplastic moulding is of great distress to the patient. Moreover, when the thermoplastic mask is produced, different parts of it are stretched by different amounts, changing its size and thickness, where potential attenuation effects are not quantified (Head, Neck and Shoulders Immobilization Systems [date unknown]; Arino et al. 2014).

The improvement of the actual construction process of the immobilisation masks as well as their configuration can lead to better health care (Li et al. 2013) experience for the patient. Also, the type of technology available for the modelling of the surfaces with the replacement of CT imaging for simpler acquisition techniques that perform better and have less radiation risks for the subjects' health are a quality gain, through the increase of the ratio benefits/risk for the patient (Kerr et al. 2017)

The main aim of the study was to evaluate the influence in the model of 3D skin surface of PIXY phantom head caused by different acquisition and reconstruction methods and to present a proposal of an alternative head immobilisation mask prototype. This preliminary solution, suited for 3D printing manufacturing, is also characterised concerning to its mechanical behaviour.

2. Materials and methods

As mentioned, in this work we will consider a set of methodologies to assess some anthropometric head measurements which will be used to understand if these approaches may constitute a viable departing point to an automated design of head immobilisation devices.

It is also intended to conclude if alternative methodologies may contribute to substitute the present conformation process of the immobilisation masks, thus avoiding the distress it causes to patients.

To this purpose, information about the geometrical characteristics of a physical phantom head (Nuclear Supplies. Pixy® Anthropomorphic Training/Teaching Phantom [date unknown]) was acquired via 3D scanning (3DS) and computerised tomography (CT), and reconstructed with different software applications.

2.1. *Acquisition equipment*

To perform the 3D scanning of the phantom head, one has used two diverse approaches. The first was based on a NextEngine laser scanning system (3DLS) in which settings involved a medium range acquisition and a number of ten sectors with a density of 132 points per square centimetre. The system precision is 0.127 mm. The second scanning system used was an Asus Xtion Pro Live based on the Primesense 3DDepth Sensor (3DDS). In this case, the camera resolution is 640 × 480 with a frame rate of 30 fps and an average accuracy of 0.5 mm, and it was used in range near mode. NextEngine scanning system generated automatically the corresponding global 3D point cloud and in the second scanning system case ReconstructMe open-source software

was used. All the measurements were also carried out with a Rosscraft Calliper with millimetric precision.

The two CTs were performed using Philips Gemini TF 16 with two different slices' thickness (1 mm and 2 mm) while keeping other acquisition parameters constant: 20 mAs, 120 kVp, pitch of 0.938, 512 × 512 pixel matrix, rotation speed of 0.5 s per rotation. The CTs were reconstructed by FBP. It is important to say that these settings are the usually considered in a normal planning CT for radiotherapy.

The CT images were next used to build the 3D head surface, using ImageJ (Zain et al. 2017; Andrey and Boudier [date unknown]). In this case, the 3D surface was obtained using ImageJ 3D Viewer plug-in by Benjamin Schmid, which uses the marching-cubes algorithm as surface reconstruction algorithm. Additionally, the use of the software Osirix (Bastos et al. 2008) has also been considered, wherein the algorithm 3D Surface Rendering Osirix Lite v. 8.0.1, with decimate-resolution of 0.10 mm, 50 iterations, for the First Surface CT Skin was considered −500 of pixel value.

In order to simplify the designation of the different models obtained, acronyms which are presented in Table 1 are considered, as well as their corresponding meaning.

In all the cases, the models were converted to a common polygonal mesh format, in order for a subsequent improvement of eventual defects, such as, for example, holes that may result from the scanning process.

All the measurements were carried out, considering the actual clinical protocols used in order to reproduce effective real procedural conditions.

2.2. *Anthropometric measures*

The different meshes obtained from the diverse acquisition approaches were subsequently imported to SolidWorks, and converted into solid entities, enabling to obtain the required measurements. Figure 1 illustrates the 3DLS and CTImg1 solid models.

The measurements carried out to characterise the anthropometry features of the physical phantom head were inspired on the set of measurements considered by Yokota (2005), taking, however, into account the minor detail of the PIXY phantom used on this study. Accordingly, and for a better illustration of these measurements' meaning, Figure 2 presents a schematic representation using one of the present models.

Table 2 complements the schematic representation in Figure 2.

Table 1. Acronyms used to identify the models.

Designation	Acquisition	Software
CTImg1	Computed tomography, 1 mm	ImageJ
CTImg2	Computed tomography, 2 mm	
CTOsx1	Computed tomography, 1 mm	Osirix
CTOsx2	Computed tomography, 2 mm	
3DLS	3D Laser scanning	NextEngine, SolidWorks
3DDS	3D Depth sensor scanning	ReconstructMe, SolidWorks

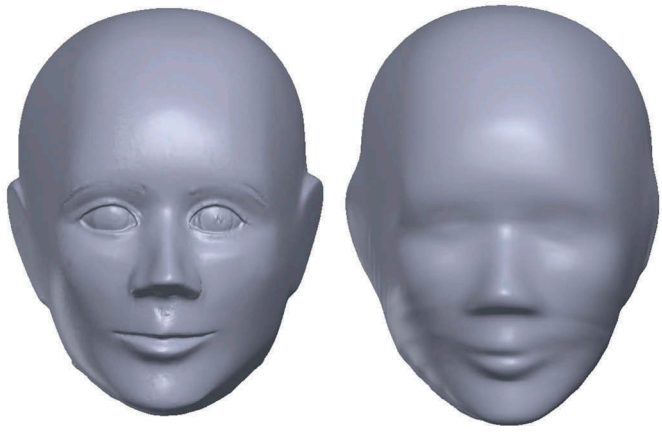

Figure 1. Solid representation of 3DLS (left) and CTImg1 (right) data.

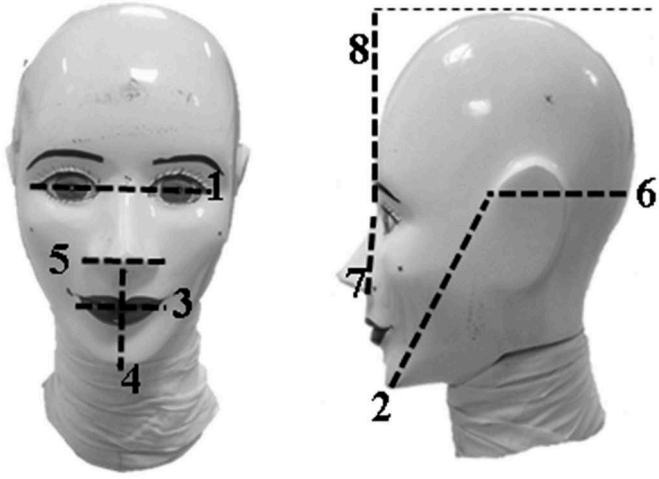

Figure 2. Schematic representation of craniofacial measurements.

After the selection of the points of interest, the measures were taken at each active layer, corresponding to a specific head computational model.

2.3. *Statistical assessment of the head models*

In the comparison of the measurements carried out to characterise the anthropometry features of the physical phantom head, one has used descriptive statistics in the first stage, namely by calculating relative deviations.

Thereafter, the statistical differences between measurements obtained within acquisitions, reconstruction methods and Rosscraft Calliper were evaluated.

In the assessment of the masks geometry, although there is not one mesh as the gold standard, it was assumed that the CT 1 mm and 3D laser scanning models may assume that role, and further tests were carried out in these two models.

Normality of the sample was evaluated with Shapiro–Wilk test to enable classifying the distribution of the samples obtained. To evaluate if there were any statistical significant differences between the measurements collected of the same landmarks, Friedman test for the multiple comparisons was applied.

Table 2. Identification of craniofacial measurements.

Measure ID	Designation	Definition
1. BIOCBRMH	Biocular breadth	Distance between the right and left ectoorbitale
2. CHINPROJ	Chin projection	XYZ coordinates between right tragion and mentona
3. LIPLGTH	Lip length	Distance between the right and left cheilion on the corner of the mouth
4. MENSUBNH	Menton–subnasal	Distance between the menton and the subnasal
5. NOSEBRTH	Nose breadth	Distance between the right and left alare
6. RTRAGX	Right tragion X	Distance between right tragion and back of the head plane
7. SBNSSELH	Subnasal-sellion length	Distance between the subnasal and sellion
8. SELLIONZ	Sellion Z	Distance between sellion and top of the head plane

All statistical analyses were performed using Statistical Package for the Social Sciences (SPSS v.24) software. For all the groups included in the study, a significance level of 5% was used (Pereira 2006).

2.4. *Material properties*

Following the geometrical models statistical assessment, it was intended to obtain a customised head immobilisation mask and to proceed to its mechanical behaviour evaluation.

To this purpose, it would be necessary to select a material that could answer to the operating conditions requisites. Therefore, a particular attention was paid to the material characteristics in terms of its mass attenuation coefficient, due to purpose. Additionally and from the manufacturing perspective, it was important also to consider the material's minimum extrusion temperature, because of the 3D printing manufacturing process that may be a serious option to consider.

Accordingly, the Polymethyl methacrylate (PMMA) was selected, and relevant properties for the present study purposes are presented in Table 3.

Table 3. PMMA material properties.

E [GPa]	ν	σ_{ys} [MPa]	ρ [g/cm^3]	*KGY*
3.3	0.43	86	1.19	1000

where E denotes the elasticity modulus, ν the Poisson ratio, σ_{ys} the yield stress, ρ the density and *KGY* corresponds to the material's tolerance level to radiation. The sources for this information were ABS Gamma Compatible Materials 2011; Material 2017; Material Property Data – MATWEB 2017.

3. Results

This section considers two main case studies, which constitute the following two sub-sections. The first case is related to the comparison and analysis of the measurements obtained for the different models and the second is focused on the mechanical performance of head immobilisation masks built from the previously obtained head models.

3.1. *Craniofacial measurements*

The results summarised in Table 4 comprehend the measurements carried out using the different methodologies, their deviations and the further statistical analysis to understand whether there are statistically significant differences among the different approaches.

It is possible to observe that there is a reasonable agreement between the values obtained using different approaches.

Considering that CT is a standard, this model was considered as reference for the relative deviation calculations' purpose. Figure 3 depicts the relative deviations of other models taking CTImgJ1 as reference.

From Figure 3 we observe that globally the CTOsx1 model is the model that presents lower relative deviations for the different anthropomorphic landmarks, followed by the 3DLS. The remaining models, CTImgJ2, CTOsx2 and 3DDS, present a worst performance, namely concerning to the ID measure 5. Excluding the case of the CTImgJ2 model, it is however relevant to say that none of the other models present deviations greater than 2.5% which is considered a good result. The measures obtained using the calliper present a greater deviation when compared with the ones associated to the 1-mm CT model reconstructed using ImageJ (CTImgJ1).

It is also important to remark that although there are some relative deviations none of them has statistically significant differences. As from the landmarks comparison obtained with the different reconstruction and/or acquisition methods, there were no statically significant differences within the methods of acquisition/reconstruction and the Rosscraft Calliper (Friedman test, X_F^2 (6)) = 6.863, p = 0.334).

These results show that statistically there is no difference in applying any of these methods for obtaining the phantom surface and for extracting landmarks measurements. However, there is a visible spatial resolution difference between the images obtained by CT and by 3DLS.

From the results it is possible to infer that probably both technologies are suited for clinical application in these procedures, allowing to avoid the exposition of the patient to extra radiation by performing many CT exams only for acquisition of the surface features. 3DLS comes as a suitable inexpensive and less harming technique for assessment of facial and body landmarks with possible clinical application utility, with great improvement in costs and in the benefit/risk ratio.

These results required further investigation for confirmation of clinic applicability, through the design and testing of masks created with the two different acquisition technologies (CT and 3DLS). To understand if this is extended to the masks design, physical and mechanical properties, these further tests are hereafter presented.

Table 4. Anthropomorphic measures obtained via different methods (mm).

Measure ID	Rosscraft Calliper	CTImg1	CTimg2	CTOsx1	CTOsx2	3DDS	3DLS
1. BIOCBRMH	85.00	86.57	86.64	86.71	86.71	86.67	86.69
2. CHINPROJ	130.00	132.65	133.57	132.51	131.67	133.36	132.30
3. LIPLGTH	55.00	54.46	54.66	54.48	54.49	54.53	54.51
4. MENSUBNH	50.00	54.85	54.05	55.19	55.59	56.39	55.11
5. NOSEBRTH	36.00	36.22	33.47	35.94	35.43	35.32	35.51
6. RTRAGX	85.00	99.85	99.78	99.80	99.98	99.60	99.93
7. SBNSSELH	50.00	50.45	50.33	50.36	50.73	51.51	50.72
8. SELLIONZ	75.00	85.69	85.73	85.70	85.68	85.73	85.69

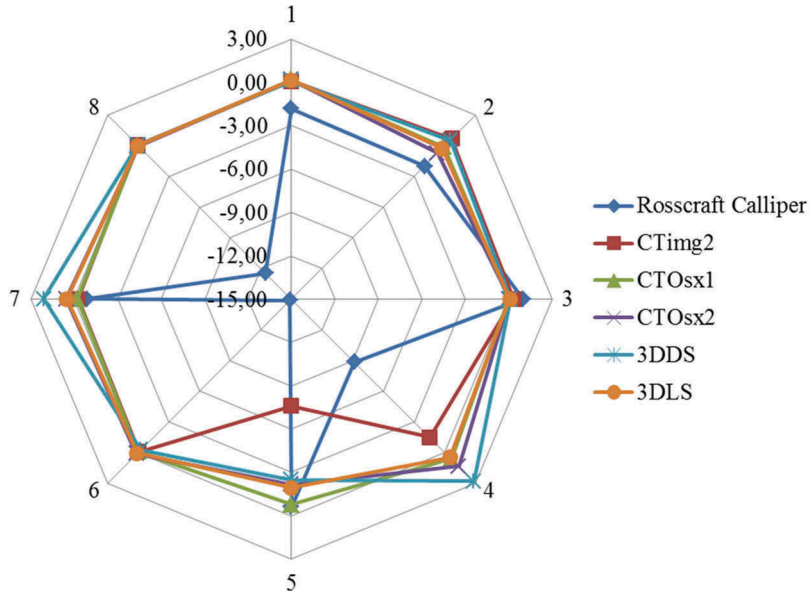

Figure 3. Relative deviations (%) of different models taking CTImgJ1 as reference.

3.2. *Immobilisation mask analysis*

From the results obtained, and considering that the 3DLS presents a good precision concerning the geometrical characterisation of the head surface and, on the other hand, the CT is widely used, it has been decided to proceed with both models to obtain the corresponding immobilisation masks. The geometrical modelling of the masks was developed in SolidWorks® (SOLIDWORKS 2018| Accelerate Innovation 2018), and the initial configurations can be observed in Figure 4, where a typical fixation to the table was selected. It is relevant to note that this fixation can be selected according to a specific table.

In order to address and contribute to a more comfortable solution concerning the claustrophobic sensations that patients may experience, an open configuration was considered (Figure 5) which was further analysed to assess its static performance. To this purpose, a set of finite element analyses were performed.

The degrees of freedom in the fixation points of the immobilisation masks to the table were constrained and a load corresponding to a more unfavourable situation was considered.

To select this situation and the magnitude of the load to impose at the masks, a left lateral bending of the neck under isometric conditions was considered with an intensity of 158.1N (Almosnino et al. 2010). This load was on the internal left side of the masks. The contact between the surface and the solid body was considered bonded. These conditions are illustrated in Figure 6 for the two masks.

It is relevant to note that this load is considered to overestimate the more probable load when patients are involved.

3.2.1. *Preliminary convergence analysis*

In order to assess the quality of the models meshes and thus to guarantee the quality of the results, a set of analyses were carried out to assess on their convergence. To this purpose, it has been considered that the masks would be built with the material with properties as presented in Section 2.4, and with thickness of 4 mm.

The results obtained both for the maximum displacement and for the maximum Von Mises stress are presented in Figure 7 and Table 5, respectively.

As one may conclude from Figure 7, the maximum displacement is convergent in both models. Table 5 presents these results and the corresponding maximum Von Mises stress which for the models presents also a convergent trend.

Accordingly, it is now possible to proceed to the static behaviour characterisation stage.

3.2.2. *Masks' static analysis*

In this study, for each of the masks, the last finite element mesh of the convergence analysis was considered. The shell

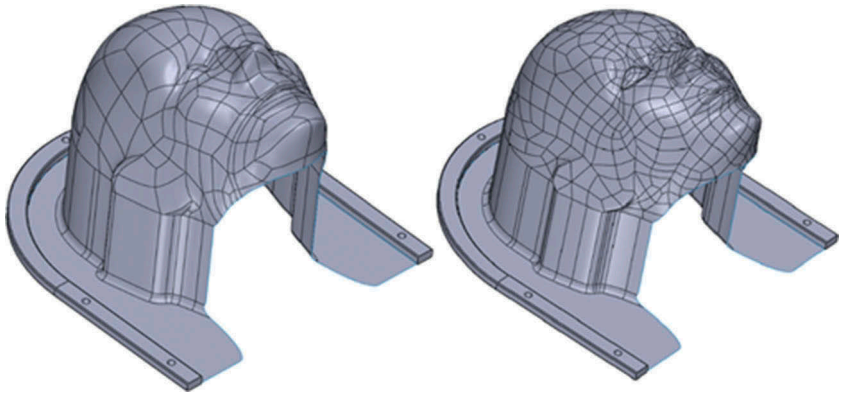

Figure 4. Full head masks corresponding to CTImg1 (left) and 3DLS (right) models.

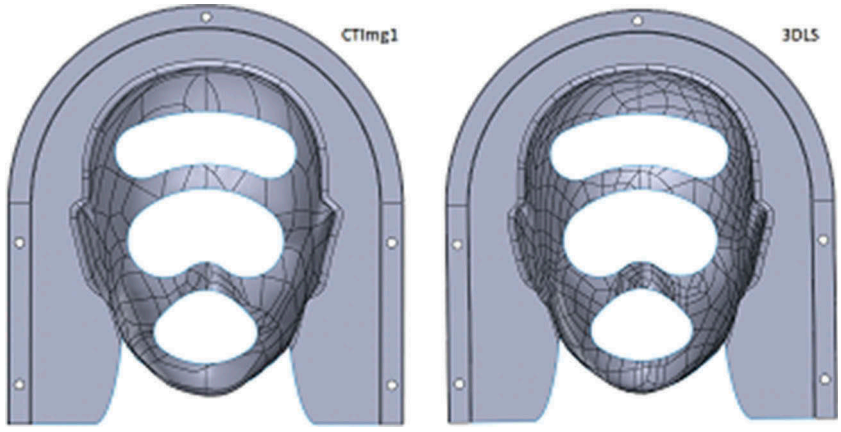

Figure 5. Open head masks corresponding to CTImg1 (left) and 3DLS (right) models.

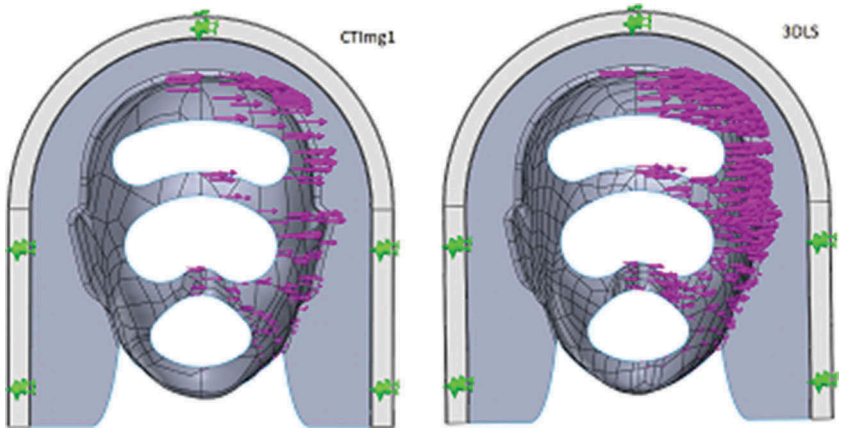

Figure 6. Free body diagrams of the head immobilisation masks (CTImg1 model on the left and 3DLS model on the right).

thickness was allowed to vary in order to analyse its influence in the static answer of the masks. For a complementary assessment of this behaviour, it was also considered that the safety factor as being the ratio between the yield stress and the maximum Von Mises stress be verified in each of the masks.

Figure 8 presents this safety factor as a function of the varying shell thickness, both for the CTImg1 and 3DLS models.

From Figure 8, it is possible to see that the mask obtained from the 3DLS head model presents a higher safety factor value in the whole thicknesses domain considered.

In correspondence to these curves, one may now observe the maximum displacement evolution as a function of the thickness, which was also analysed. These results are relevant as they are related to the stiffness of the mask.

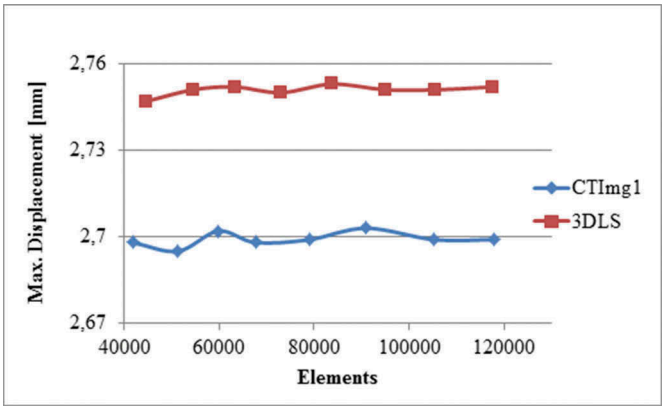

Figure 7. Maximum displacement convergence analysis.

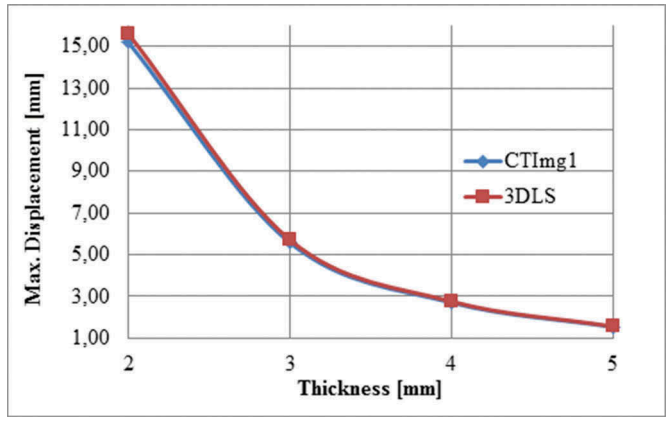

Figure 9. Maximum displacement vs. thickness for the head masks.

Table 5. Maximum displacement and maximum von Mises stress convergence analyses.

	CTImg1 mask			3DLS mask	
Elements	Von Mises Stress [MPa]	Displacement [mm]	Elements	Von Mises Stress [MPa]	Displacement [mm]
41842	12.86	2.698	44603	11.35	2.747
51264	12.77	2.695	54417	13.04	2.751
59789	13.37	2.702	63299	13.06	2.752
67636	12.90	2.698	72981	12.42	2.750
78933	12.97	2.699	83768	13.29	2.753
90933	13.43	2.703	95064	12.32	2.751
105376	13.08	2.699	105540	13.84	2.751
117953	13.49	2.699	117520	13.03	2.752

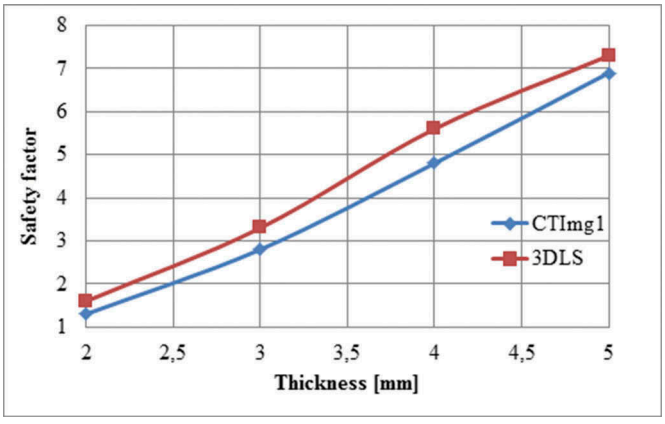

Figure 8. Safety factor vs. mask thickness.

For immobilisation purposes, it is considered adequate to have a maximum displacement around one millimetre; so this analysis took that value as a goal, results being convergent, as depicted in Figure 9.

For a better illustration of the displacements verified in the masks for an arbitrary mask thickness, Figure 10 presents this distribution for the 3DLS mask considering a 4 mm thickness.

As a final remark related to Figures 9 and 10, a consistent result is registered among the different quantities analysed; one verifies that the safety factor increases with the thickness and the corresponding maximum displacement decrease. Concerning to the maximum Von Mises stress, one sees that it decreases at the same time the masks become stiffer and the immobilisation becomes higher.

4. Discussion

This study intended to evaluate the possibility of considering alternative approaches to obtain head immobilisation masks for therapeutic and diagnosis purposes. To this purpose, different acquisition strategies were considered to obtain the corresponding phantom head computational models to which anthropometric relevant measures were further assessed. The measurements were also infirmed with the physical measurements by Rosscraft Calliper, an additional available measurement tool (Gribel et al. 2011) although with known less accuracy when compared with the other techniques used.

The results obtained allowed to understand that although all the measurements for 3D reconstructions acquired with all methods are similar, the Rosscraft Calliper measurements were very different in some cases. The marks that present higher dissimilitude as we can see clearly in Table 4 are ID measures 6 and 8. Despite these deviations, it was possible to conclude from the Friedman test that no statistically significant differences were found for the global measures set.

These differences were probably due to the different level of precision and accuracy that were obtained in the other techniques when compared with the physical measurements obtained with Rosscraft Calliper, as it has not so high resolution as the used software for the reconstructed measurements (Coward et al. 2005).

While the reference points of measurements in the reconstructed images were the same creating good accuracy and precision, the physical measurements performed with the Rosscraft Calliper had less precision in the choice of the reference point of measurement for the absence of well-established reference points, being this a source of less accuracy in the physical measurements to add to the low precision level of the calliper used (Gribel et al. 2011).

When compared with all the reconstructed methods, these did not present statistically significant differences, and all the relative deviations obtained were inferior to 15% for any reference method chosen, allowing us to conclude that all

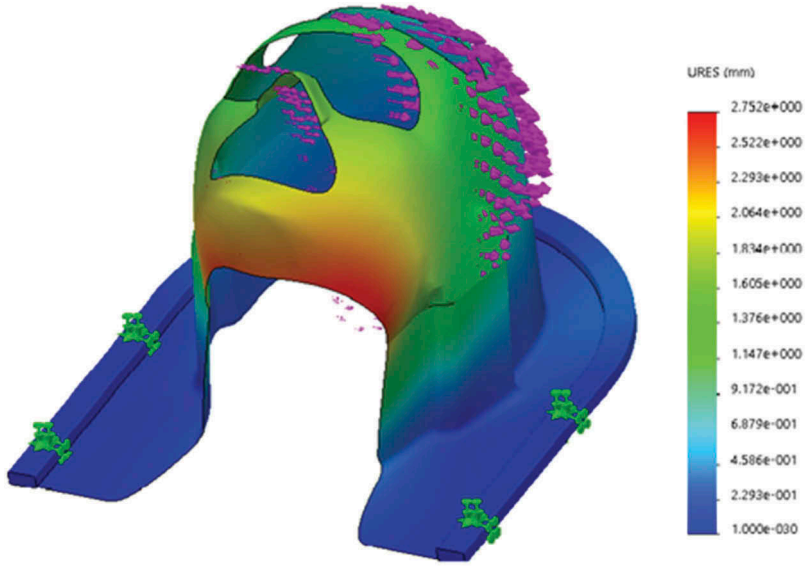

Figure 10. Maximum displacement for 3DLS mask with 4 mm thickness.

methods from a statistical point of view are suitable for the reconstruction process; this is consistent with other studies already published that also proved overall consistency between these techniques in the measurements of faces (Kau et al. 2005; Kaim et al. 2009).

In CT-based models, although the reconstruction algorithms perform with similar characteristics of accuracy in the reconstruction, slice thickness is proved to add an increased influence factor by degrading the spatial resolution. The well-known influence of acquired slices thickness in the image quality of the CT is visible between the comparisons of different CT reconstruction methods with the same slices thickness, and between the comparison of acquisitions with different slices thickness with the same method (Kau et al. 2005; McNitt-Gray 2006; Kaim et al. 2009).

Likewise, the reconstruction methods effects of the CT images were more evidently observed in the comparison of the ImageJ reconstruction with the Osirix reconstruction for the lower resolution acquired CT (2 mm) (Coward et al. 2005; Kau et al. 2005; McNitt-Gray 2006; Kaim et al. 2009).

This study also considered the geometrical modelling of an immobilisation mask adapted to two head computational models obtained both from computerised tomography and laser scanning. The mask model intends to be a preliminary contribution to a customised automated manufacturing process and to this purpose it was necessary to address both material attenuation coefficient requirements as well as mechanical ones, namely concerning to the mask stiffness and strength. In this context, and in order to address the necessary radiotransparency, it was considered that the mask would be made of polymethyl methacrylate (Gamma Compatible Materials 2011).

The two mask models, based on the tomography acquisition and on the laser scanning acquisition, were initially submitted to preliminary studies in order to ensure the quality of the respective meshes.

The mechanical performance of the mask models was finally assessed considering an unfavourable loading condition, corresponding to a left lateral bending of the neck under isometric conditions (Almosnino et al. 2010). The results obtained are considered very favourable from the immobilisation perspective, being also guaranteed that the maximum equivalent Von Mises stress stays far behind the material yield stress.

5. Conclusions

From the studies developed in the present work, it is possible to conclude that from a statistical point of view, all the generated head computational models can be considered suitable for the head anthropometric measures characterisation.

Based on this first conclusion, it is therefore possible to equate the automated design of customised head immobilisation devices based on any of the three-dimensional surfaces acquisition approaches.

To illustrate this, a mask prototype is proposed based on two of the acquisition approaches considered: the CT and the laser scanning. In any case, a material that would respect radiotransparency pre-requisites and also an effective mechanical behaviour that is able to ensure the necessary immobilisation was adopted.

As a final global conclusion, one may say that the present immobilisation mask design proposal may be an effective alternative to the present completely hand-made situation, which presents a high-degree of discomfort and stress to the patients.

Acknowledgements

The authors wish to acknowledge the financial support of Project IPL/2016/SoftImob/ISEL, IPL/2016/*CardiaCor*_ESTeSL and Project LAETA—UID/EMS/50022/2019. The authors also wish to acknowledge Fundação Champalimaud for the possibility of obtaining the CT images which were essential to this study.

Disclosure Statement

No potential conflict of interest was reported by the authors.

Funding

The authors wish to acknowledge the financial support of Project IPL/2016/SoftImob/ISEL, IPL/2016/CardiaCor_ESTeSL and Project LAETA—UID/EMS/50022/2019.

Notes on contributors

MAR Loja is with GIMOSM, ISEL/IPL, Grupo de Investigação em Modelação e Optimização de Sistemas Multifuncionais, and with LAETA, IDMEC, Instituto Superior Técnico. Her academic background integrates PhD in Mechanical Engineering. Her research interests are related to the areas of Computational Mechanics of Solids, Optimization and Reverse Engineering.

E Sousa is with GI-MOSM, ISEL/IPL, Grupo de Investigação em Modelação e Optimização de Sistemas Multifuncionais and, H&TRC – Health &Technology Research Center, ESTeSL/IPL - Escola Superior de Tecnologia da Saúde de Lisboa/Instituto Politécnico de Lisboa. Her academic background integrates MSc in Biomedical and Biophysical Engineering. Her research interests are related to the areas of Medical Image and Radioteraphy.

L Vieira is with GI-MOSM, ISEL/IPL, Grupo de Investigação em Modelação e Optimização de Sistemas Multifuncionais, H&TRC – Health &Technology Research Center, ESTeSL/IPL - Escola Superior de Tecnologia da Saúde de Lisboa/Instituto Politécnico de Lisboa and, Instituto de Biofísica e Engenharia Biomédica, Faculdade de Ciências da Universidade de Lisboa, Lisboa, Portugal. Her academic background integrates PhD in Biomedical and Biophysical Engineering. Her research interests are related to the areas of Medical Image and Radioteraphy.

DMS Costa is with GIMOSM, ISEL/IPL, Grupo de Investigação em Modelação e Optimização de Sistemas Multifuncionais. His academic background integrates a MSc in Mechanical Engineering. His research interests are related to the areas of Smart Structures, FEA, Multifunctional Materials and Optimization.

R Parafita, Medical Physicist of Nuclear Medicine-Radiopharmacology, Champalimaud Centre for the Unknown, Champalimaud Foundation, MSc in Physics Engineering, Interests in Medical Image and Radiation Protection

DC Costa, Director of Nuclear Medicine-Radiopharmacology, Champalimaud Centre for the Unknown, Champalimaud Foundation; Nuclear Medicine Physician; MSc and PhD by the University of London, UK; Fellow of the Royal College of Radiologists, London, UK; Emeritus Reader, University College London, London, UK; past-President of UEMS-EBNM (from 2012 to 2015).

ORCID

MAR Loja http://orcid.org/0000-0002-4452-5840
E Sousa http://orcid.org/0000-0003-4181-0192
L Vieira http://orcid.org/0000-0002-7109-6535
R Parafita http://orcid.org/0000-0001-6986-1552
DC Costa http://orcid.org/0000-0001-8039-4924

References

Abramoff MD, Viergever MA. 2002. Computation and visualization of three-dimensional soft tissue motion in the orbit. IEEE Transactions on Medical Imaging. 21(4):296–304. http://ieeexplore.ieee.org/document/1000254/.

Almosnino S, Lucie P, Joan MS. 2010. Retest reliability of force-time variables of neck muscles under isometric conditions. J Athl Train. 45(5):453–458.

Amato ACM. 2017. Surface length 3D: plugin Do OsiriX Para Cálculo Da Distância Em Superfícies. Jornal Vascular Brasileiro. 15(4):308–311. http://www.scielo.br/scielo.php?script=sci_arttext&pid=S1677-54492016000400308&lng=pt&tlng=pt.

Andrey P, Boudier T. [date unknown]. 3D processing and analysis with ImageJ. [accessed 2018 Mar 20]. https://pdfs.semanticscholar.org/858c/f348b692a34b2075cc1ef577be08c2344ea1.pdf.

Anguelov D, Koller D, Srinivasan P, Davis J, Thrun S, Pang HC. [date unknown]. The correlated correspondence algorithm for unsupervised registration of nonrigid surfaces. Stanford AI Lab Technical Report SAIL2004-100. [accessed 2018 Mar 20]. https://ai.stanford.edu/~drago/Papers/cc.pdf.

Arino C, Stadelmaier N, Dupin C, Kantor G, Henriques De Figueiredo B. 2014. Le Masque de Contention En Radiothérapie : Une Source D'anxiété Pour Le Patient ? Cancer/Radiothérapie. 18(8):753–756. http://linkinghub.elsevier.com/retrieve/pii/S1278321814003643.

Bastos EO, Goldenberg DC, Fonseca A, Kanashiro E, Yoshida M, Alonso N. 2008. Osirix: Uma Estação de Trabalho Radiológica Portátil Ao Alcance Do Cirurgião. Rev Soc Bras Cir Craniomaxilofac. 11(1):27–31.

Bernardo GMS, Loja MAR. 2017. Reconstruction and analysis of hybrid composite shells using meshless methods. International Journal of Advanced Structural Engineering. 9(2):111–128.

Bernardo GMS, Rodrigues JA, Loja MAR. 2016. Towards an expeditious as-is surface reconstruction. Engineering Structures. 129:91–107. http://linkinghub.elsevier.com/retrieve/pii/S0141029616313177.

Coward TJ, Scott BJ, Watson RM, Richards R. 2005. A comparison between computerized tomography, magnetic resonance imaging, and laser scanning for capturing 3-dimensional data from an object of standard form. Int J Prosthodont. 18(5):405–413. https://www.ncbi.nlm.nih.gov/pubmed/16220806.

Dodziuk H. 2016. Applications of 3D printing in healthcare. Polish Journal of Cardio-Thoracic Surgery. 3:283–293.

Douros I, Dekker L, Buxton BF. 1999. An improved algorithm for reconstruction of the surface of the human body from 3D scanner data using local B-spline patches. In: Proceedings IEEE international workshop on modelling people. MPeople'99, IEEE Comput. Soc. p. 29–36. http://ieeexplore.ieee.org/document/798343/.

Gamma Compatible Materials. 2011. Nordion – science advancing health. [accessed 2018 Mar 20]. http://www.nordion.com.

Gopan O, Wu Q. 2012. Evaluation of the accuracy of a 3D surface imaging system for patient setup in head and neck cancer radiotherapy. International Journal of Radiation Oncology*Biology*Physics. 84(2):547–552. http://linkinghub.elsevier.com/retrieve/pii/S0360301611036595.

Gribel B, Gribel M, Frazão D, McNamara J, Manzi F. 2011. Accuracy and reliability of craniometric measurements on lateral cephalometry and 3D measurements on CBCT scans. Angle Orthodontist. 81(1):26–35. https://www.ncbi.nlm.nih.gov/pubmed/20936951.

Head, Neck and Shoulders Immobilization Systems. [date unknown]. [accessed 2018 Apr 20]. https://www.orfit.com/radiation-oncology/products/ahead-neck-and-shoulders/.

Kaim AH, Kirsch EC, Alder P, Bucher P, Hammer B. 2009. Preoperative accuracy of selective laser sintering (SLS) in craniofacial 3D modeling: comparison with patient CT data. Rofo. 181(7):644–651.

Kau CH, Richmond S, Zhurov AI, Knox J, Chestnutt I, Hartlesf F, Playleg R. 2005. Reliability of measuring facial morphology with a 3-dimensional laser scanning system. Am J Orthod Dentofacial Orthop. 128(4):424–430.

Kerr W, Rowe P, Pierce SG. 2017. Accurate 3D reconstruction of bony surfaces using ultrasonic synthetic aperture techniques for robotic knee arthroplasty. Computerized Medical Imaging and Graphics. 58:23–32. http://linkinghub.elsevier.com/retrieve/pii/S0895611117300204.

Li G, Lovelock DM, Mechalakos J, Rao S, Della-Biancia C, Amols H, Lee N. 2013. Migration from full-head mask to 'open-face' mask for immobilization of patients with head and neck cancer. Journal of Applied Clinical Medical Physics. 14(5):243–254.

Material ABS. 2017. Eurapipe duraflo. [accessed 2018 Mar 20]. http://xahax.com/subory/Spec_ABS.pdf.

Material Property Data – MATWEB. 2017. MatWeb. [accessed 2018 Apr 20]. http://www.matweb.com/index.aspx.

McNitt-Gray MF. 2006. Tradeoffs in CT image quality and dose. Medical Physics. 33(6):2154–2155.

Morton AM. 2011. Validation of 3D surface measurements using computed tomography. [dissertation]. Kingston, Ontario: Queen`s University, School of Computing.

Nuclear Supplies. Pixy® anthropomorphic training/teaching phantom. [date unknown]. Auckland: globalMedical solutions, nuclear supplies. [accessed 2017 Jul 10]. http://www.nuclearsupplies.co.nz/pdfs/anthropomorphicphantoms.pdf.

Paquet E, Rioux M 2003. Antropometric visual data mining: a content based approach. International Ergonomics Association XVth Triennial Congress; 2003 August 24–29; Seoul, Korea. https://nparc.nrc-cnrc.gc.ca/eng/view/object/?id=6851e262-f2f0-4c80-96e8-b3f61198a453.

Pereira A. 2006. SPSS Guia Prático de Utilização Análise de Dados Para Ciências Sociais E Psicologia. Lisboa: Edições Sílabo.

Richard S, Husarik DB, Yadava G, Murphy SN, Samei E. 2012. Towards task-based assessment of CT performance: system and object MTF across different reconstruction algorithms. Medical Physics. 39(7Part1):4115–4122.

SOLIDWORKS 2018 | Accelerate innovation. 2018. SOLIDWORKS. [accessed 2018 Mar 10]. https://www.solidworks.com/.

Yokota M. 2005. Head and facial anthropometry of mixed-race US army male soldiers for military design and sizing: a pilot study. Applied Ergonomics. 36(3):379–383. http://linkinghub.elsevier.com/retrieve/pii/S0003687005000347.

Zain RM, Razali AM, Salleh KAM, Yahya R. 2017. Image reconstruction of x-ray tomography by using image J platform. In: AIP Conference Proceedings. 1799. AIP Publishing pp. 050010-050010-6. http://aip.scitation.org/doi/abs/10.1063/1.4972944